Jül-Conf-45 D4-3

I C A N S - V
MEETING OF THE INTERNATIONAL COLLABORATION ON
ADVANCED NEUTRON SOURCES
June 22-26, 1981

Some Remarks Concerning the Use of a Rotating W-Target in a High Power Spallation Neutron Source

G.S. Bauer*, W. Lohmann* and F. Stelzer**

* Institut für Festkörperforschung
** Zentralabteilung für Allgemeine Technologie
Kernforschungsanlage Jülich
D-5170 Jülich, Fed. Rep. Germany

Abstract

In this paper we show that a rotating target for a high power spallation neutron source using tungsten as a target material can be built relatively easily and operated safely. According to experimental results we do not expect a significant disadvantage to result from the use of W instead of Pb even for the D_2O-tank of the hybrid moderator system proposed for the target station DIANE in the SNQ concept. We therefore conclude that the use of a rotating W-target is a viable backup solution for the SNQ target concept, avoiding practically all of the yet to investigate difficulties with a canned target material.

1. Introduction

For the spallation neutron source proposed in Germany, the initial moderator concept chosen consists of a D_2O-tank and an H_2O-moderator with lead reflector arranged above and below a rotating target /1/ as shown in Fig. 1. Since it was felt that the time average neutron flux in the D_2O depended quite critically on losses by absorption, a target concept was developed which allowed the use of the only weakly absorbing lead in conjunction with Al as structural material. Due to the thermal and thermomechanical properties of lead (low melting point, poor thermal conductivity, large differential expansion, low flow stress etc.) it was decided that the target should be built of about 9000 cylinders individually canned in aluminium /2/ and cooled by water flowing between them (see Fig. 1). Another incentive to choose this concept was - and still is - to make possible a later transition to uranium as target material and provide a safe containment for the then present fission products. Extensive studies /3/, /4/, /5/ have shown that such a concept should be feasible, but there remain a few problems which could not yet be investigated in sufficient detail to give a reliable estimate of the expected lifetime of such a target. Apart from this, the design has the following drawbacks:

- Difficult manufacturing procedure;
- dilution of target material by cooling channels and cladding material;
- need for a window to contain the coolant. This window, although rotating with the target, is the most heavily loaded part of the structure as far as radiation effects are concerned;
- mechanical load on the structure due to coolant pressure;
- part of the cooling water is hit by the proton beam, which may enhance corrosion effects.

These problems - and hence their possible effects on the target lifetime - can be avoided if tungsten is used as target material as shown in the present note. Table 1 summarizes some important properties of tungsten.

Density (g/cm^2)	19.3
Hardness H_V (swaged material) (N/mm^2)	4600 - 7500
Tensile strength (swaged material) (N/mm^2)	1500 - 5000
*Young's modulus (20°C) (N/mm^2)	400.000
Melting point (K)	3683
*Thermal conductivity (20°C) (W/cm K)	1.7
*Coefficient of thermal expansion (20K) (K^{-1})	$4.4 \cdot 10^{-6}$
Ductile-brittle transition (K)	400 - 700
Thermal neutron absorption cross section (barn)	19.2
Mean free path for protons of 1.1 GeV (cm)	9.8
Range of protons of 1.1 GeV (cm)	36

Table 1 Some properties of tungsten

*see also Figures

2. Design principle of the rotating tungsten target

As will be shown in section 3, it is sufficient to cool the upper and lower surface of a tungsten ring used as target with the SNQ-parameters[1] to remove the heat dissipated in the target even from the most highly loaded regions. This makes a target design possible, as sketched in Fig. 3. For manufacturing reasons and also to reduce internal stresses, the target consists of a large number of (almost) close packed hexagonal rods. (Of course it would be tolerable also to use square cross sections). Small gaps are left between the rods to accomodate lateral thermal expansion. In order to ensure good thermal contact, these rods are tightly bonded to the upper and lower support plates which contain the cooling channels. Since the coolant is flowing only in these bores, there results no bending stress on the support plates as in the design of Fig. 1. The proton beam does not hit the coolant directly and hence no window to contain the coolant is needed. A number of ways to arrange the coolant channels are conceivable in addition to the one shown in Fig. 3. It is possible to provide several separate sections which are only mechanically connected to one another, and thereby facilitate the manufacturing of the target wheel. Because of the short range of protons in tungsten, it is sufficient to have a target depth of 35 cm rather than 70 cm as required for the Pb-target of the reference concept, thereby reducing the number of target elements and hence the cost. According to manufacturers' quotes, one target element (rod) of the tungsten target would cost about as much as an Al-canned lead target element. Together with the much simpler manufacturing procedure of the whole target, this may result in considerable savings. The target has a high degree of mechanical rigidity due to the tight bonding between the target elements and the support structure.

3. Thermal and mechanical load on the rotating W-target

For the sake of simplicity, the geometry used earlier /3/ to calculate the temperatures and stresses in the lead target was also used for the W-target elements. This means, that a cylindrical rod of 24 mm diameter and 100 mm length, hit by a proton beam symmetrical to its centre plane once every two seconds (time of revolution of the target) was considered. The finite element method was used, and for symmetry reasons only one half of a rod at the outer periphery of the wheel was modelled. The grid of nodes and finite elements is shown in Fig. 2. For the sake of convergency it was necessary to use thin elements in the region of the heat sink. Within each nodal plane, a subdivision was made into 48 elements (65 nodal points) for which the time-dependent temperatures and stresses were computed. The heat deposition in the target was assumed to decrease purely exponentially along

---

[1] Outer target diameter 2,5 m; Height of target 10 cm; Frequency of rotation 0,5 Hz; Proton pulse repetition rate 100 Hz; Proton beam diameter 4 cm FWHM; Peak proton current 100 mA (1.1 GeV); Proton pulse duration 0,5 ms.

the proton beam with a decay constant given by the protons' mean free path (Table 1) and to follow in its lateral distribution the profile of the proton beam. This profile was assumed to be gaussian with a FWHM of 4 cm in both directions and truncated at 8 cm. The total heat deposition was assumed to be approximately the same as in a Pb-target /6/. The time-dependent temperature after startup is shown in Fig. 4 for the hot spot and for the first 30 revolutions of the target wheel. At this point equilibrium has almost been reached and the mean temperature can be seen to be about 350 K above the coolant temperature (i.e. about 680 K). The temperature cycling is 44 K once every two seconds.

For this first set of calculations the thermal conductivity and heat capacity have been assumed as temperature independent, using values of 1.5 W/cm•K and 130 J/kg•K respectively. From Figs. 7 and 8 it can be seen that this is not exact, but in view of the large distance of the operating temperature from the melting point, this is not very important. The distributions of reference stresses and maximum temperatures in the most highly stressed plane are shown in Figs. 5 and 6. The peak stress of 20.9 N/mm² is far below the tensile strength which is 3400 N/mm² (Fig. 9). Thus, even the fact that the operating temperature is above the ductile-brittle transition should not be important.

The maximum difference in thermal expansion (Fig. 10) between two target elements (separated by 4 cm, i.e. next nearest neighbours) is 0.01 mm on either side of the rods. There is no difficulty expected in accomodating this in the support plates.

From a thermomechanical point of view it seems that the use of a W-target as described here is absolutely without problems. All loads, at least in the unirradiated material, are far from any critical values.

4. Effect of irradiation on the performance of the rotating W-target

The kind and the amount of radiation damage in the rotating target is mainly determined by the intermittent proton irradiation and the time-averaged fast neutron flux. Table 2 shows some material parameters of W concerning the damage due to protons and neutrons.

	σ_{dpa} (barn)	σ_{He} (barn)	σ_{H} (barn)
Protons (800 MeV)	9100	0.58	5.13
Neutrons (E>0.1 MeV)	173 (fission spectrum)	$0.32 \cdot 10^{-3}$ (fusion spectrum)	$0.7 \cdot 10^{-3}$ (fusion spectrum)

Table 2 Radiation damage cross sections for proton- and neutron irradiation of W. The threshold energy for atomic displacement is assumed to be E_d = 65 eV.

The proton data are taken from calculations using a proton energy of 800 MeV. This does not seem to be very crucial for a first material assessment. The neutron data have been generated in the case of the dpa-damage by averaging over a FBR-spectrum, in the case of the gas production by averaging over a fusion reactor spectrum in order to take the harder spallation neutron spectrum into consideration. The latter values are therefore an upper limit for the expected damage.

Using the data from Table 2, values for the dpa-damage and the gas production under the SNQ operations conditions have been calculated and are given in Table 3. The spatial maximum of the time average fast neutron flux was estimated as $1.8 \cdot \hat{\Phi}$ (Pb)*, corresponding to the neutron yield ratio, Y(W)/Y(Pb) = 0.9 and the twofold shorter mean free path of protons in W.

	dpa-damage rate (dpa/sec)	He-production rate (appm He/sec)	H-production rate (appm H/sec)
Protons	$1.63 \cdot 10^{-7}$	$1.02 \cdot 10^{-5}$	$9 \cdot 10^{-5}$
Neutrons	$1.4 \cdot 10^{-8}$	$2.5 \cdot 10^{-8}$	$5.5 \cdot 10^{-8}$

Table 3 Radiation damage data for a rotating W-target.

Proton irradiation parameters: E_p = 800 MeV, $\bar{I}$ = 5 mA, FWHM = 4 cm

Neutron irradiation parameter: $\hat{\Phi}(W) = 7.9 \cdot 10^{13}$ $cm^{-2}s^{-1}$ (E>0.1 MeV)

Obviously, the damage created by the neutrons can be neglected nearly completely. Assuming - as for the SNQ reference design - a target working time of two years (12.000 h), the peak total damage is expected to be

7.6 dpa; 440 appm He; 3.900 appm H.

For proton irradiation of W, 1 mAh/cm² equals 0.21 dpa, 13 appm He and 115 appm H.

Furthermore, Re is created as a solid transmutation product from (n,γ)-reactions of the isotopes W^{184} and W^{186} with thermal neutrons. This Re-enrichment should give no problems because of the good alloyability of Re with W and several favourable properties of W-Re alloys (see below).

We are not aware of results from high energy proton irradiations of W. Therefore, for an assessment of the irradiation induced property changes, results from neutron irradiations were used. Because n-irradiated samples have a very low gas content, statements concerning the effects of the estimated He- and H-concentrations are not possible directly. As an outcome of the generally high H-mobility in metals, one can expect a noticeable H-release at the operating temperature level (section 3). For He, one has a quite different release behaviour. Thermal desorption measurements on He-implanted samples indicate the onset of He-release from surface layers (5 Å) at temperatures above 600°C,

* $\hat{\Phi}$(Pb) as calculated in ref. /6/ is $4.4 \cdot 10^{13}$ $cm^{-2}s^{-1}$ for E > 0.1 MeV

whereas He-release from the bulk is not observed below 1500-2100°C /7/. In order to estimate the possible He-induced material deteriorations like bubble swelling or embrittlement, an investigation of material containing roughly 500 appm He (cyclotron-injected) seems to be necessary. On the other hand, one can get - applying W made by powder metallurgical methods (product density below the theoretical density of W) - a product with a more open structure, providing a catching volume for the gaseous spallation products.

The findings concerning the void swelling are positive throughout. The SNQ-operating conditions will probably not lead into the void swelling region of W after two years of operation (Fig. 12). Even if this should occur, the amount of the void swelling will be very small. For pure W, only 0.25% after 9.5 dpa have been measured (Fig. 13). As can also be seen from Fig. 13, this may be diminished further by alloying. Higher, but absolutely tolerable void swelling values are reported for a n-irradiation of a W single crystal: after 3.9 dpa at 450-500°C a density of 1.2% is observed /10/.

The irradiation induced mechanical property changes of W have not been investigated in great detail. Results of tensile tests on wrought and stress-relieved material, which has been n-irradiated to 1.6 dpa at 385°C /11/, indicate trends which are typical of metals: with increasing dose the tensile strength increases, whereas the ductility decreases. Compared with the unirradiated condition, the gain in strength (expressed by the increase of the yield strength) at the SNQ-operating temperature of 400°C is about 57% after 1.6 dpa (Fig. 14, upper part). As a measure of the ductility loss, the total elongation decreases to roughly 45% of the unirradiated value (Fig. 14, lower part), which corresponds to absolutely about 4%.

Whereas the strength increase caused by the irradiation can be considered as very favorable, the drop in ductility might seem a serious problem at the first glance. Based on the magnitude of the thermomechanical stresses (section 3), the resulting strains are close to 10^{-3}, which lies far away from the critical limits. Furthermore, the intrinsically brittle behaviour of W has to be taken into account anyway in the design, especially because of the relatively high ductile-brittle transition temperature (DBTT). The DBTT values quoted in Table 1 can be lowered by alloying (e.g. with Re) or by a high degree of cold work (Fig. 15). These precautions may be necessary in order to keep the operating temperature within the ductile range, because the DBTT is shifted to higher temperatures under irradiation. In the paper mentioned above /11/, an DBTT-increase from -65°C to 230°C after 1.6 dpa is found. For W in the recrystallized condition, a DBTT-shift from 315°C to 793°C is observed already after 0.1 dpa /13/.

Summarizing, one can state, that the effects of the radiation damage after two years of operation are foreseeable and manageable. The void swelling can be neglected. The changes of the mechanical properties seem to be only weakly dose-dependent after about 0.5 dpa. The strength increase by irradiation hardening gives no problems. On the other hand, the accompanying ductility losses as well as irradiation-induced DBTT-increase should be investigated experimentally under damage conditions typical of the SNQ. Such data are necessary for a final materials selection, especially with regard to alloying and processing. In this context, a more detailed investigation of the change of the materials properties due to the relatively high He-concentration would also be desirable.

Based on the present knowledge, highly cold-worked W-products made by powder metallurgical methods - possibly alloyed with Re - offer the best characteristics for an application as SNQ target material.

5. Neutronic performance of a spallation neutron source with W-target

In order to get a feeling for the effect on the performance when replacing the lead target by a tungsten target in the target station DIANE of the SNQ-concept (i.e. with the hybrid moderator arrangement), a few measurements were carried out at the Swiss Institute of Nuclear research /14/. For a proton energy of 600 MeV, the following results were obtained:

(1) No difference was found for the thermal neutron leakage from the fast moderator. For this measurement both targets had been "diluted" by placing polyethylene sheets between the bricks from which they were put together (10% by volume). Omitting this dilution in the case of tungsten is expected to result in a 10 to 15% gain. Russell et al /15/ have found a 15% advantage for a small W-target over a lead target at 800 MeV.

(2) In a volume of D_2O (170x170x85 cm^3 LxWxH) located underneath the target, the thermal neutron flux distributions shown in Fig. 16 were found using Dy-foil activation. Obviously there is a much stronger flux depression near the target for tungsten, as expected from its high absorption cross section. On the other hand, the maximum flux value is reduced by 15% only and is shifted farer away from the target. For a cold neutron source of 30 cm height and located with its bottom about 10 cm above the bottom of the D_2O-tank /1/, the loss in time average flux will certainly be less than 10%. Also, it can be assumed that this loss in time average flux does not show up in the peak flux but only in a faster decay due to absorption.

These first results, although still incomplete and of preliminary nature, show, that the backup solution proposed here - although not applicable to a uranium target - is a viable one to ensure safe and reliable operation of the DIANE target station.

6. Use of the rotating W-target with a proton compressor for a pulsed source

As a second stage in the SNQ-concept it has been proposed to build a pulsed neutron source by introducing a proton pulse compressor. This compressor, called IKOR (isochronous compressor ring) /16/ is designed to deliver 0.7 μs long pulses of an integrated intensity ($2.7 \cdot 10^{14}$ protons) which amounts to 83% of that delivered in the basic concept within 500 μs. This results in extremely short heating times and hence is likely to lead to shock-waves in the target. According to a paper by Sievers /17/, a criterion as to whether or not such shock waves arise can be derived from the time a sound wave takes

to travel through the part of height 2B of the target element heated by the pulse of duration t_p. If

$$c \cdot t_p \leq 2B,$$

a temperature rise by ΔT_o results is a stress level

$$\sigma_o = E \cdot \alpha \cdot \Delta T_o$$

(E = Young's modulus, α = coefficient of thermal expansion).

If

$$c \cdot t_p \geq 2B,$$

one obtains

$$\sigma_{max} = \sigma_o \cdot \frac{2B}{c \cdot t_p} .$$

Making the simplifying assumption that the heat deposition is constant over a section 2B = 4 cm of the target rod, some data have been compiled in Table 4 for a Pb-target element with AlMg3-canning and for a W-target rod. The value of $3.6 \cdot 10^5$ N/cm² used for W corresponds to a temperature of 700 K (see Fig. 11).

Material	$\alpha(10^{-6}k^{-1})$	$E(\frac{N}{mm^2})$	$c \cdot t_p$(cm)	ΔT_o(K)	$\sigma_{max}(\frac{N}{mm^2})$	$\sigma_{zul}(\frac{N}{mm^2})$ *
Pb	29.1	$1.3 \cdot 10^4$	0.07	36	13.6	1-6
AlMg3	23.8	$7.1 \cdot 10^4$	0.43	21	35.5	60-120
W	4.6	$3.6 \cdot 10^5$	3.0	37	61.3	100-460**

* Endurance limit for alternating load

**Swaged material at 10^8 load cycles

Table 4 Data for the maximum stresses in the target of a pulsed source of the SNQ-concept

From Table 4 it can be seen, that in the case of a Pb-target the dynamic stresses are higher than the endurance limit under the assumed conditions, while there remains a clear safety margin in the case of tungsten. It should

be noted that this estimate is somewhat pessimistic on the one hand and that the stresses are of compressive nature on the other, which does relax the situation to some extent. Hence it may be concluded that a rotating W-target should also be applicable to a pulsed neutron source in the SNQ-concept.

7. Conclusions

The concept of a rotating W-target outlined in this paper is suitable for the basic intensity modulated SNQ concept (target station DIANE) as well as for a possible future pulsed source. The flux penalty in the D_2O-tank is acceptable, whilst it may be anticipated that, for 1.1 GeV proton energy, there is a gain in the H_2O-moderator due to the shorter range of the protons in tungsten relative to lead. This concept bypasses a number of difficulties present in the reference concept due to the fact that cooling of the upper and lower target surface alone is sufficient. Although not suited for a transition to uranium, it constitutes a viable backup solution for day one operation of a high power spallation neutron source.

References:

/1/ G.S. Bauer
"Layout of the Target Station for the German High Power Spallation Neutron Source Project"
Proc. ICANS IV-meeting, report KENS II (1981) pp. 156-180

/2/ H. Stechemesser and G.S. Bauer
"Engineering, Activity Handling and Emergency Considerations for a Rotating High Power Target"
Proc. ICANS IV-meeting, report KENS II (1981) pp. 313-322

/3/ E. Graudus, A. Sievers und F. Stelzer
"Temperaturen und Spannungen in den zylinderförmigen Protonentargets der Spallations-Neutronenquelle"
unpublished report KFA Jülich, ZAT-Bericht Nr. 110-II-22

/4/ E. Graudus, A. Sievers und F. Stelzer
"Berechnung und Optimierung des Targetradgehäuses der Spallations-Neutronenquelle"
unpublished report KFA Jülich, ZAT-Bericht Nr. 104-II-21

/5/ W. Lohmann
"Materials Problems in Beam Windows and Structural Compounts of the SNQ-Target"
Proc. ICANS IV-meeting, report KENS II (1981) pp. 323-332

/6/ G.S. Bauer, H. Sebening, J. Vetter and H. Willax, eds.
"Realisierungsstudie zur Spallations-Neutronenquelle"
Part I available as report Jül-Spez 113 and KfK 3175 (1981)

and

G.S. Bauer
"Einige Vorüberlegungen zur Targetstation einer Spallations-Neutronenquelle"
unpublished internal report KFA Jülich, KFA-PSN-IB 1/79 (1979)

/7/ G. Farrell and W.A. Grant
"Radiation Damage in Tungsten: Its Influence on the Trapping and Subsequent Thermal Desorption of Helium"
rad. eff. 3 (1970), 249

/8/ V.K. Sikka, J. Moteff
"Treshold Temperature for Void Formation in the Group VIa Metals"
Trans. Am. Nucl. Soc. 16 (1973), 97

/9/ J. Matolich, H. Nahm and J. Moteff
"Swelling in Neutron Irradiated Tungsten and Tungsten-25 Percent Rhenium"
Scr. Met. 8 (1974), 837

/10/ V.N. Bykov, G.A. Birzhevoi and M.I. Zakharova
"Change in the Density of Single-Crystal Tungsten During Neutron Irradiation"
At. Energ. (USSR) 32 (1972), 323

/11/ J.M. Steichen
"Tensile Properties of Neutron Irradiated TZM and Tungsten"
J. Nucl. Mat. 60 (1976), 13

/12/ W.D. Wilkinson, in
"Properties of Refractory Metals", New York (1969), p. 165

/13/ C.L. Younger and G.N. Wrights
"Effect of Reactor Irradiation on Ductile-Brittle Transition and Stress-Strain Behavior of Tungsten"
NASA-Report, Sept. 1970

/14/ G.S. Bauer, H.M. Conrad, F. Gompf, H. Spitzer und W. Reichardt
"Neutronenausflüsse aus wasserstoffhaltigen Moderatoren einer Spallations-Neutronenquelle für verschiedene Geometrien und Materialkombinationen des Target-Moderator-Reflektorsystems"
unpublished report in part III of the SNQ study

/15/ G.J. Russell, M.M. Meier, J.S. Gilmore, R.E. Prool, H. Robinson and A.D. Taylor
"Measurement of Spallation Target-Moderator-Reflector Neutronics at the Weapons Neutron Research Facility"
Proc. ICANS V-meeting, report KENS II (1981)

/16/ The IKOR study group:
"IKOR, An isochronous compressor ring for proton beams"
G. Schaffer, ed.
report Jül-Spez-114 (1981)

/17/ P. Sievers
"Elastic Stress Waves in Matter Due to Rapid Heating by an Intense High Energy Particle Beam"
unpublished internal report CERN (1976)

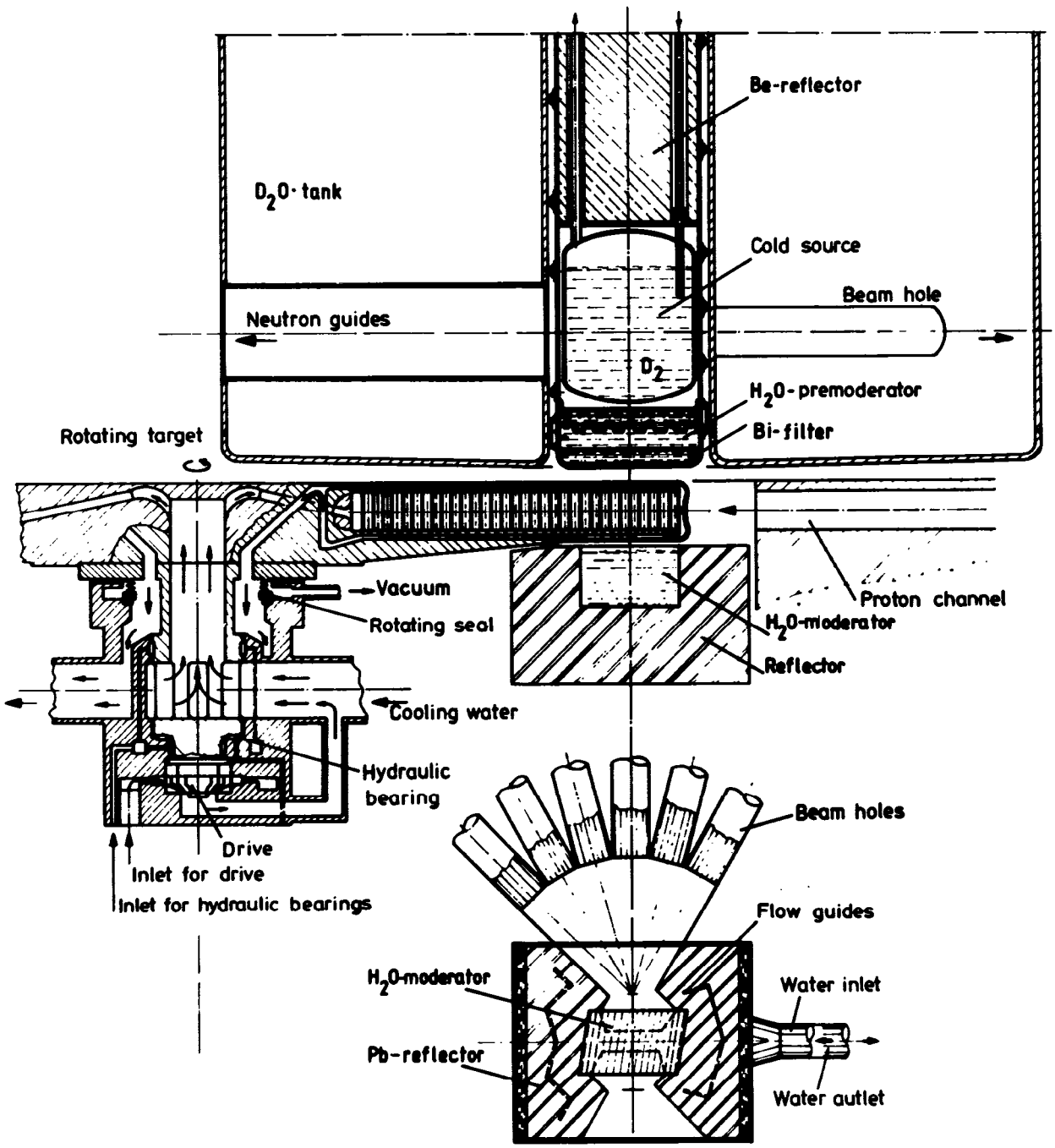

Fig. 1 Target-moderator arrangement as proposed for the SNQ target station DIANE. The individual target elements are directly cooled by water flowing between them and returning to the hub of the wheel through the upper and lower support structure.

Materials constant: Temperature independent thermal conductivity: 1.5 W/cmK

volume heat capacity: $\rho \cdot c = 2.5/J/cm^3K$

Young's modulus and thermal expansion temperature dependent

maximum heat density: 211 kW/cm³ (during pulse)

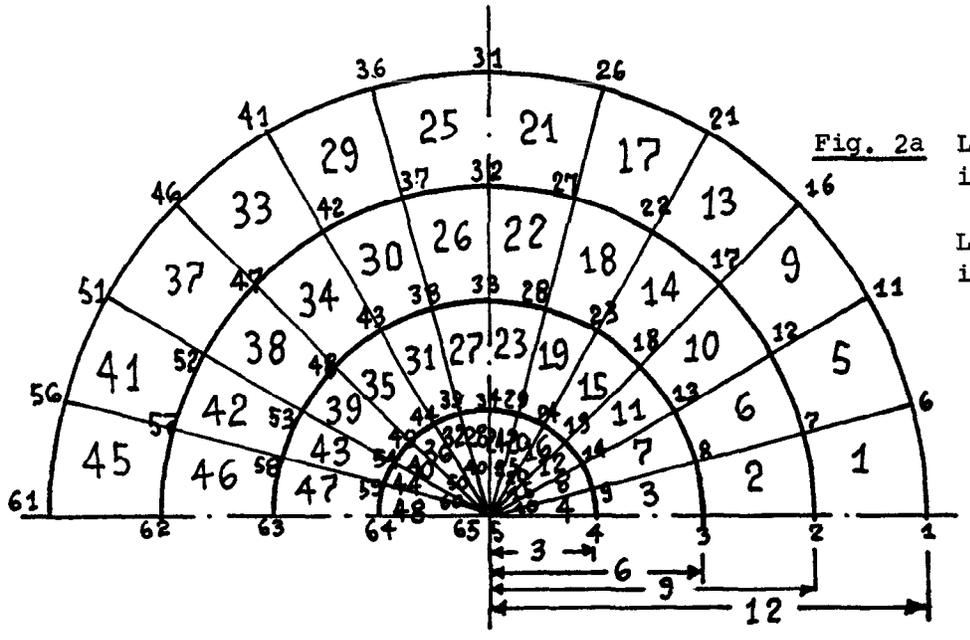

Fig. 2a Labelling of nodes in nodal plane 1

Labelling of elements in level 1

total of 288 elements and 455 nodes.

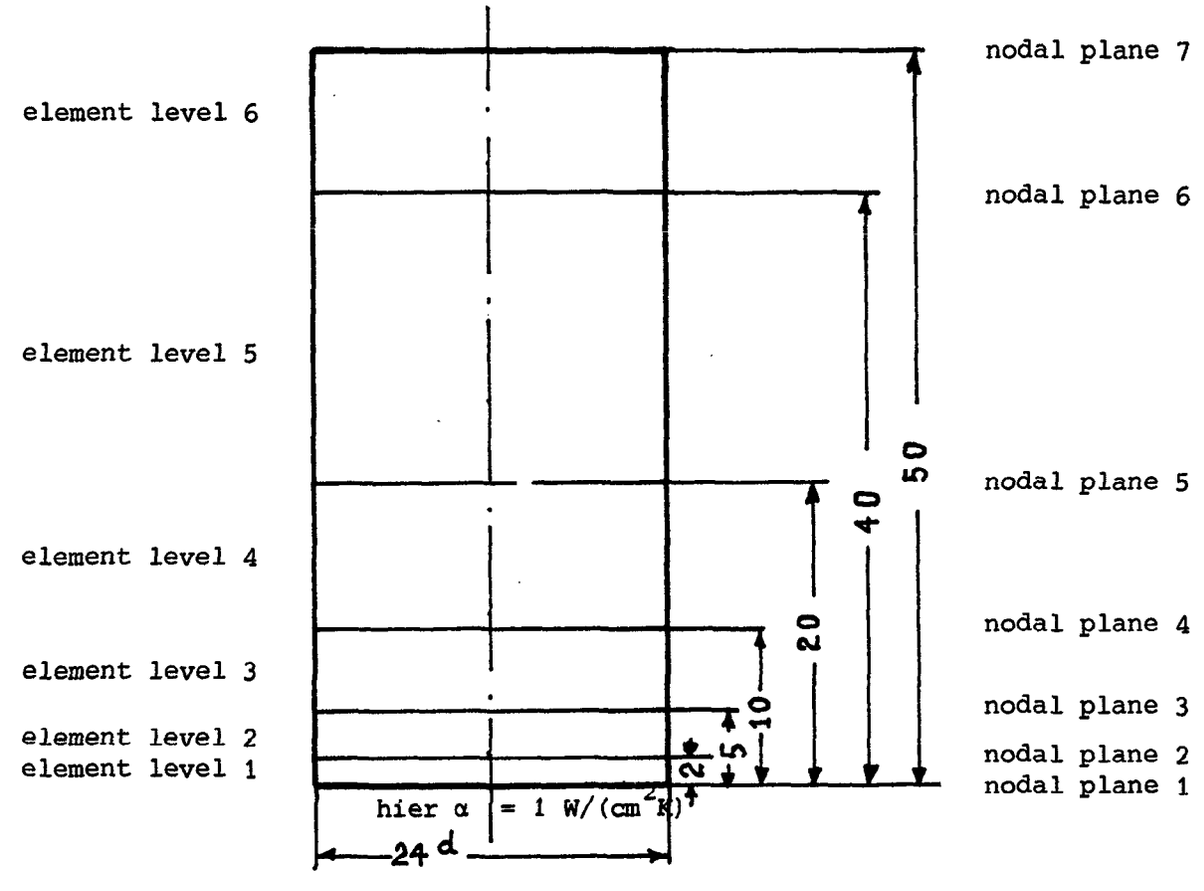

Fig. 2b Dimensions used for the mathematical model.

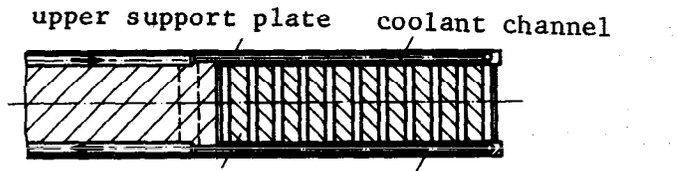

a) Vertical Section

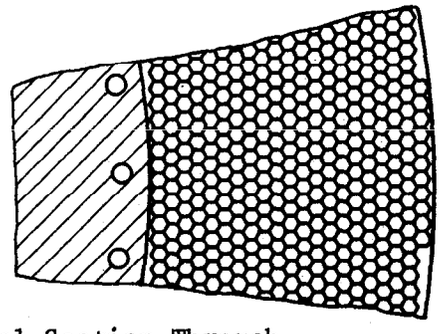

b) Horizontal Section Through Target Centre Plane

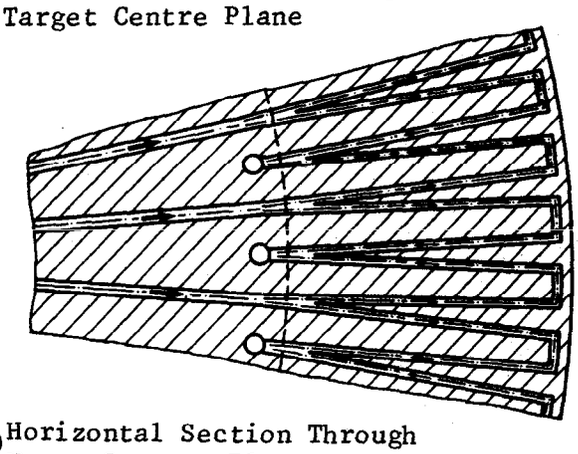

c) Horizontal Section Through Upper Support Plate

Fig. 3 Target region of a rotating W-target. Coolant flows only in the support structure, not between the hexagonal target elements.

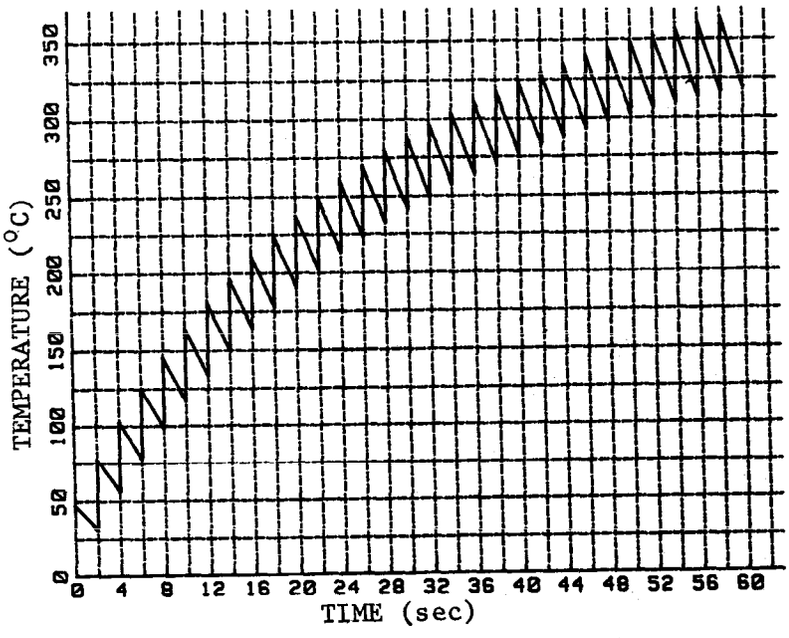

Fig. 4 Time dependence of temperature at the hot spot after start-up of the source at full power (node 391).

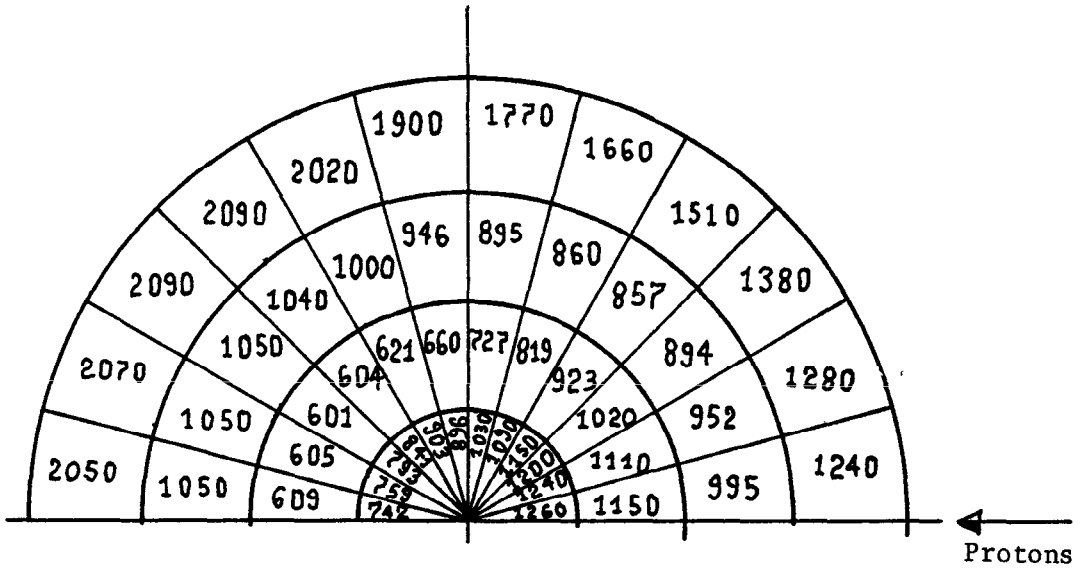

Fig. 5 Reference stresses in N/cm² in element level 6, the most highly stressed level, after 30 revolutions. The tensile strength of W at the temperature in question is about 340.000 N/cm².

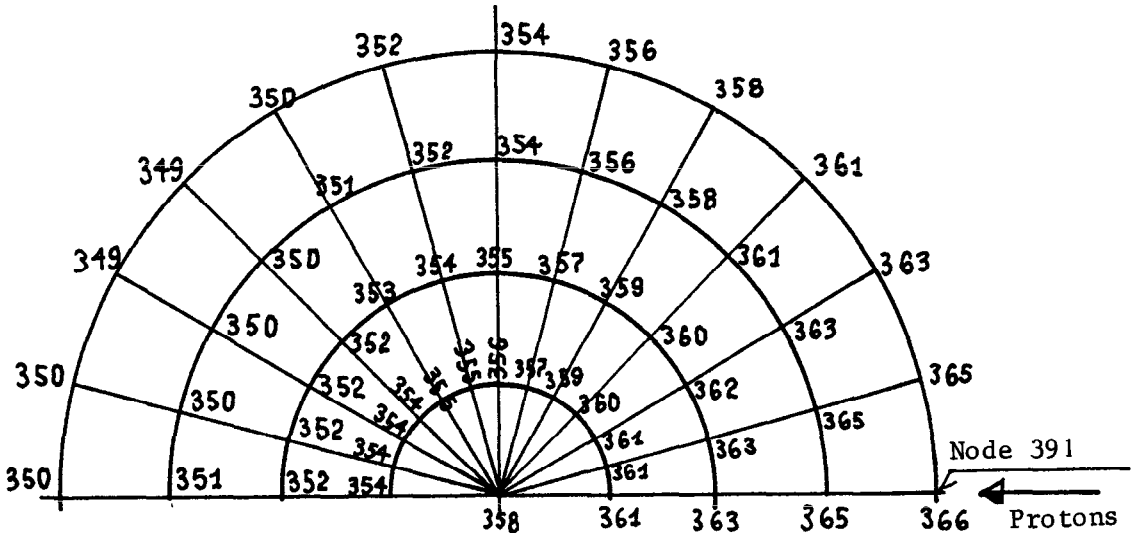

Fig. 6 Temperatures at the nodes of nodal plane 7 after 30 revolutions of the target wheel. This is the plane showing the highest temperatures.

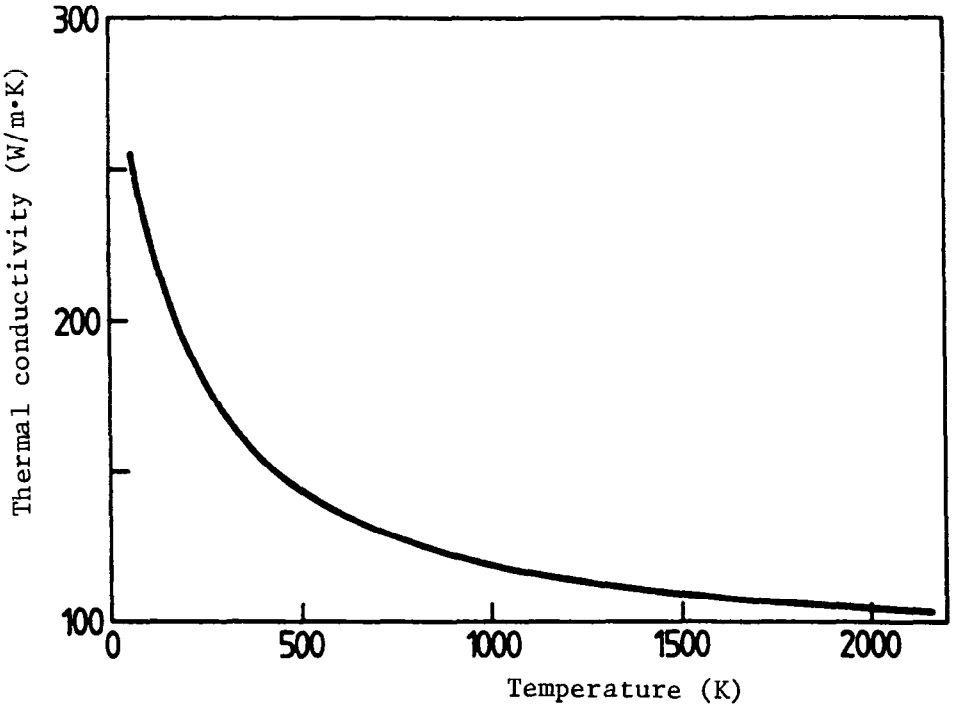

Fig. 7 Thermal conductivity of tungsten as a function of temperature.

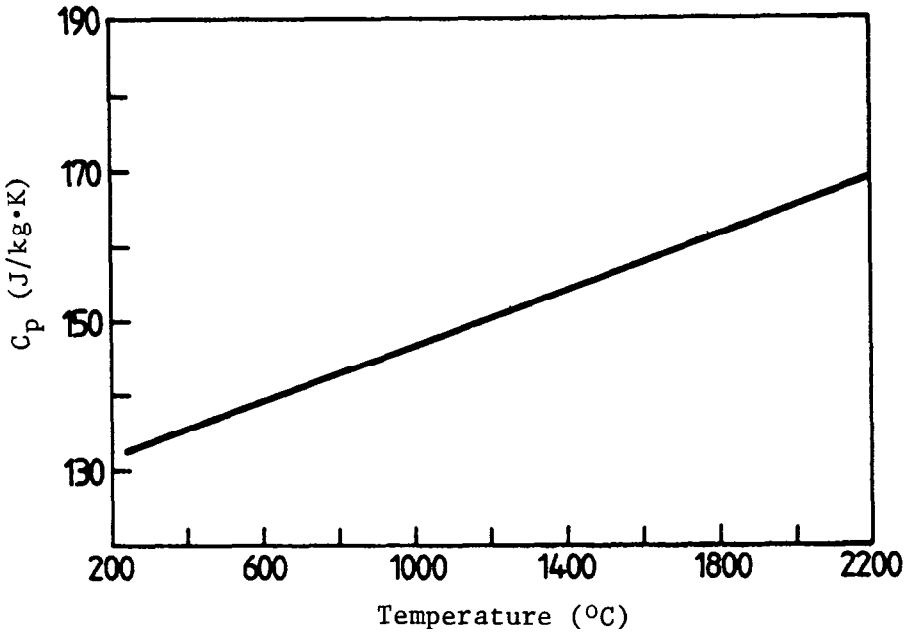

Fig. 8 Specific heat capacity of tungsten as a function of temperature.

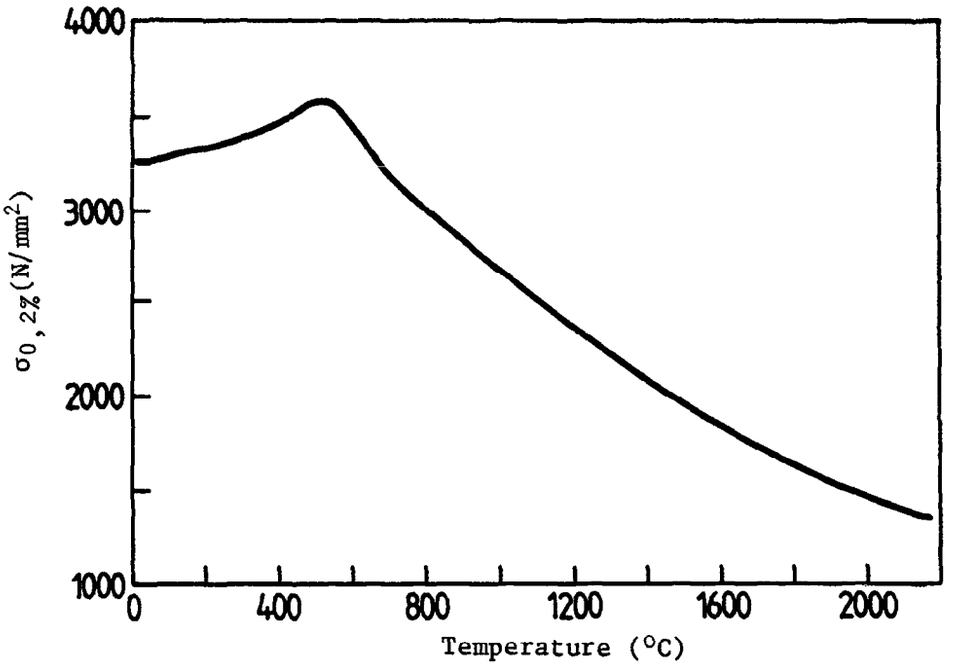

Fig. 9 Yield stress of tungsten as a function of temperature.

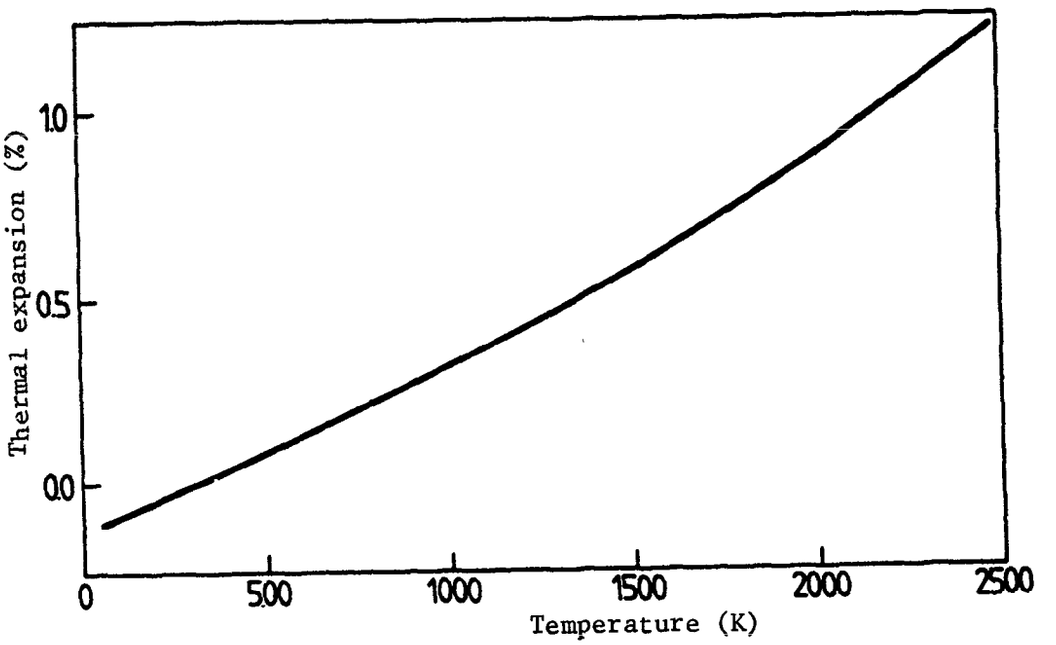

Fig. 10 Linear thermal expansion of tungsten between 0°C and T.

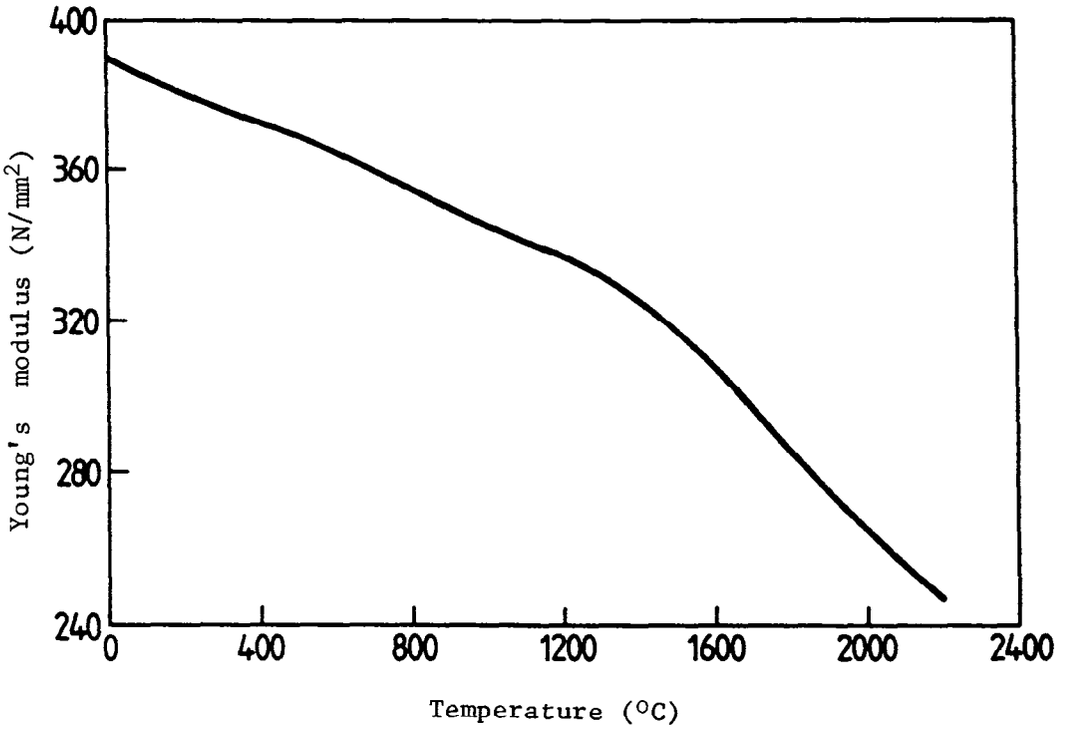

Fig. 11 Young's modulus of tungsten as a function of temperature.

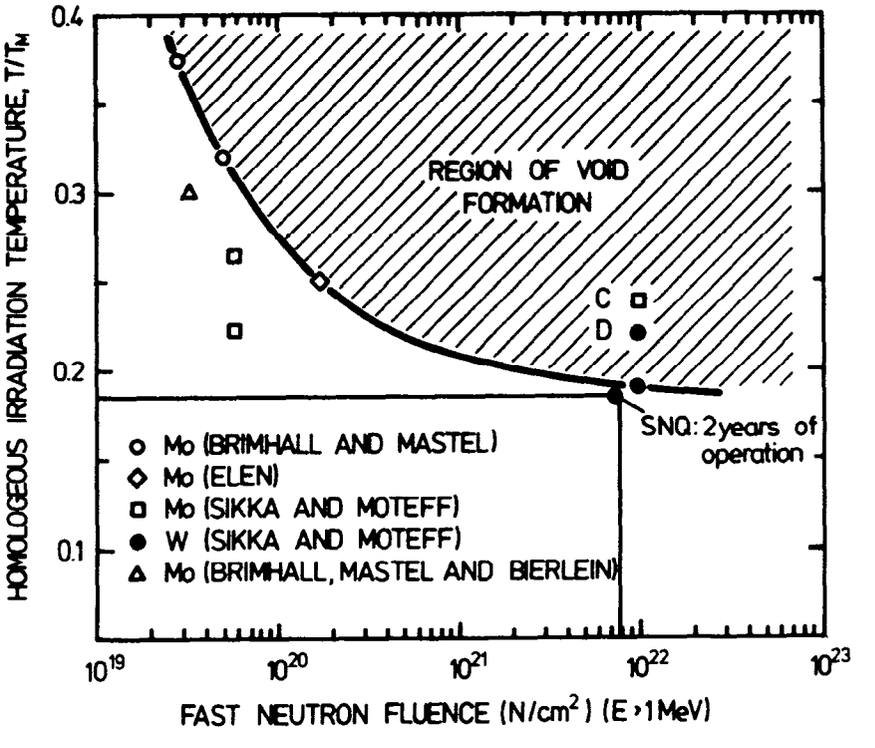

Fig. 12 Temperature- and fluence dependence of the void formation in the group VIa refractory metals /8/. The expected damage of 7.6 dpa after two years of operation corresponds to roughly $7.8 \cdot 10^{21}$ n/cm^2 (E > 1 MeV). For a temperature of 680 K = 0.18 • T_m, the region of void formation is not reached.

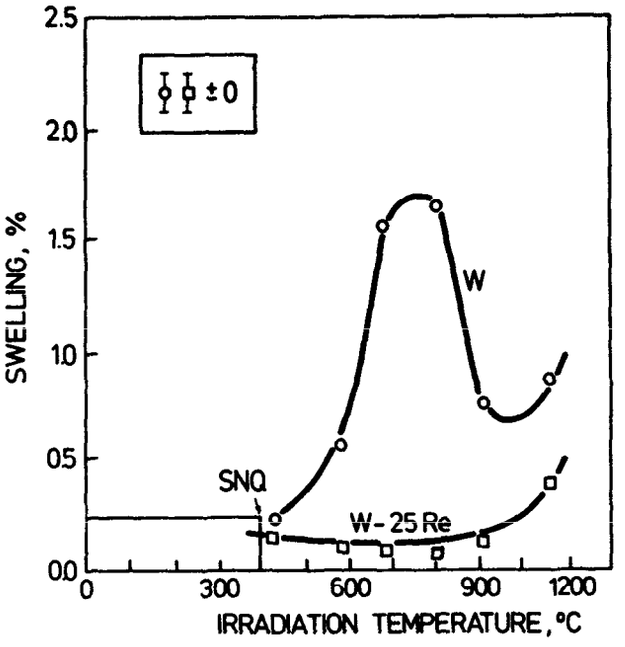

Fig. 13 Swelling of irradiated W (O) and W-25 Re (□) after 9.5 dpa as a function of temperature /9/. The SNQ operating temperature of about 410°C lies far away from the peak swelling temperature.

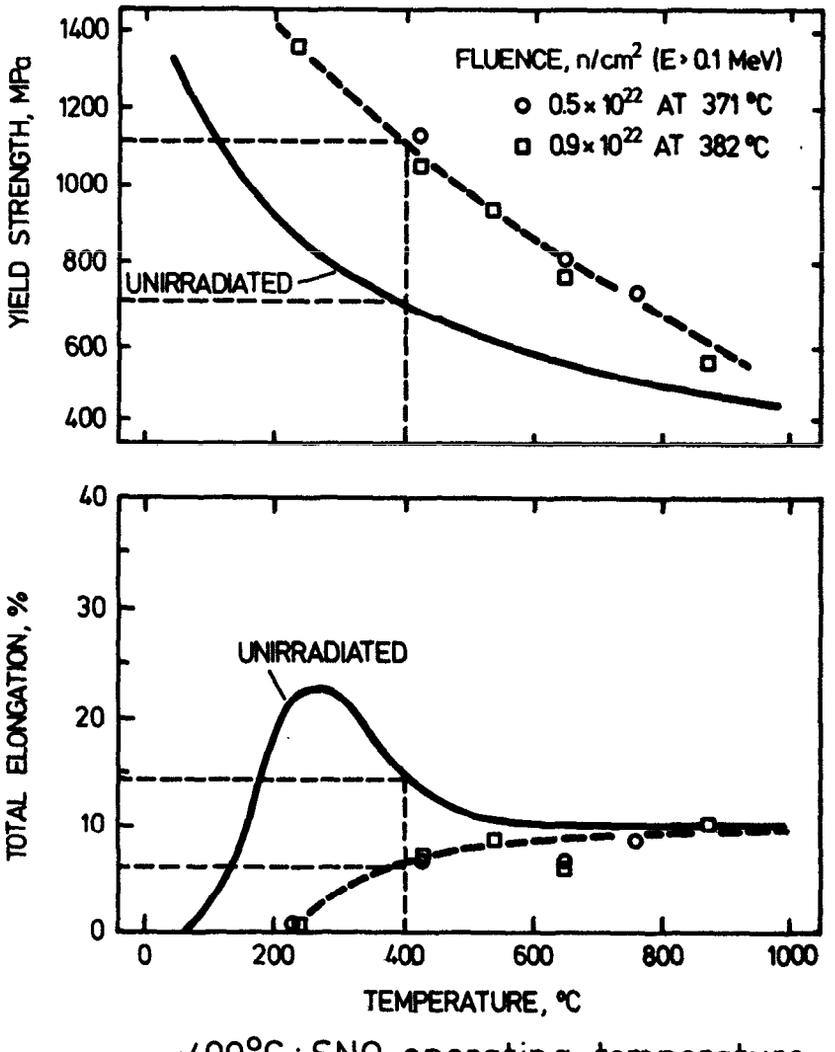

Fig. 14 Temperature dependence of strength (upper part) and ductility (lower part) of unirradiated and irradiated (1.6 dpa at 385°C) tungsten /11/.

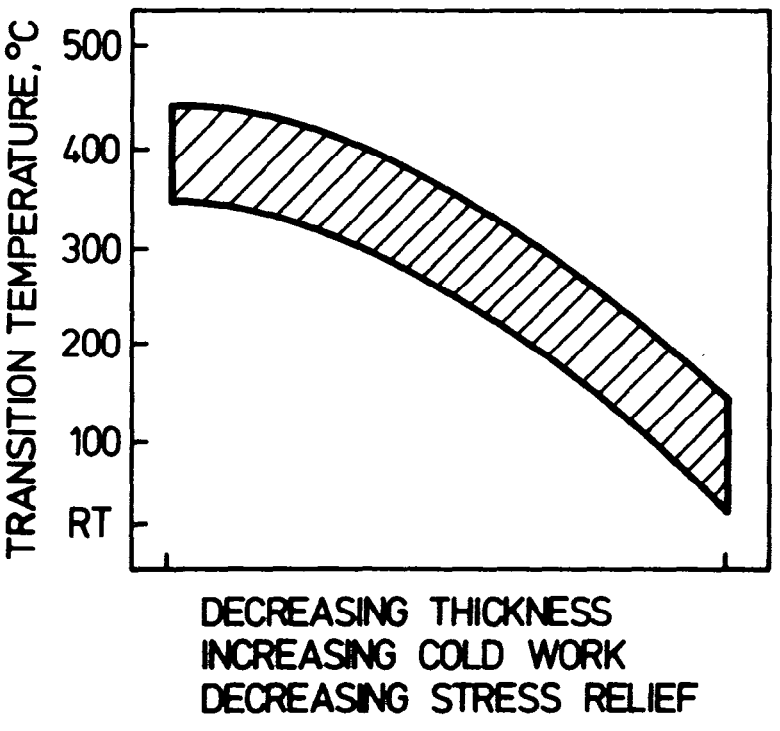

Fig. 15 Influence of processing parameters on the ductile-brittle transition temperature of flat-rolled, powder-metallurgy tungsten products /12/.

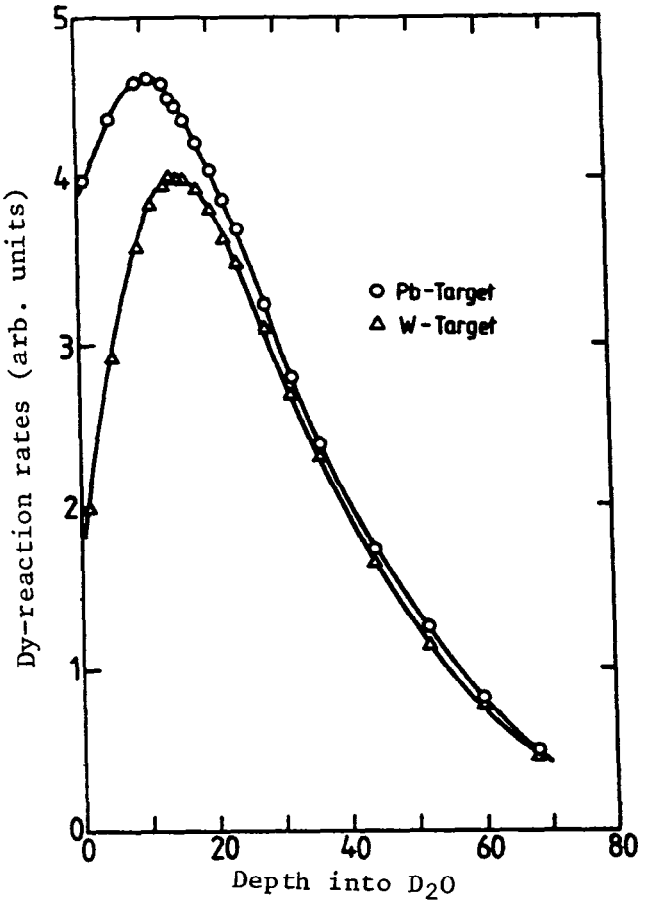

Fig. 16 Comparison of measured thermal neutron flux distribution in a D_2O-tank located below targets of Pb resp. W. Proton energy was 600 MeV.